Sigma-Delta Receive Beamformer Based on Cascaded Reconstruction for Ultrasound Imaging Application

Jia Hao Cheong, Yvonne Ying Hung Lam, Kei Tee Tiew, and Liang Mong Koh

***Abstract*—A pre-delay reconstruction sigma-delta beamformer (SDBF) was recently proposed to achieve a higher level of integration in ultrasound imaging systems. Nevertheless, the high-order reconstruction filter used in each channel of SDBF makes the beamformer highly complex. The beamformer can be simplified by reconstructing the signal after the delay-and-sum process with only one filter. However, this post-delay reconstruction-based design degrades image quality when dynamic focusing is performed. This paper shows that employing a simple pre-delay filter is sufficient to achieve similar performance as conventional pre-delay reconstruction SDBF, as long as the pre-delay filter provides the required pre-delay signal-to-quantization noise ratio (SQNR). Based on this finding, we proposed a cascaded reconstruction beamformer that uses a boxcar filter as the pre-delay filter in each channel. Simulations using real phantom data demonstrate that the proposed beamforming method can achieve a contrast resolution comparable to that of the pre-delay reconstruction beamforming method. In addition, the hardware can be greatly simplified compared with the pre-delay reconstruction beamformers.**

I. Introduction

Ultrasound beamforming has extensively shifted into the digital domain due to the processing flexibility and the ease of handling crosstalk and noise problems [1]. The image quality has greatly been improved as a result of the enhanced delay accuracy. However, high-speed multi-bit analog-to-digital converters (ADC) and front-end digital circuitries are required to achieve the necessary delay accuracy. To mitigate the high speed requirement of ADCs, an interpolation beamformer (IBF) and a quadrature demodulation (QD) based phase rotation beamformer (PRBF) have been developed and have come into common use [2]. Although IBF and PRBF relieve the sampling frequency of the ADC, a computationally expensive finite impulse response (FIR) filter is required in each channel (as interpolation filter for IBF and demodulation filter for QD-based PRBF). The expensive FIR filter in each channel makes the design of ultrasound systems challenging, especially for large channel count systems (e.g., 3-D ultrasound machines) as well as for low-cost hand-held systems.

Manuscript received June 29, 2007; accepted March 10, 2008.

The authors are with the Division of Circuits and Systems, School of Electrical and Electronic Engineering, Nanyang Technological University, Singapore (e-mail: cheo0030@ntu.edu.sg).

Digital Object Identifier 10.1109/TUFFC.885

To reduce the hardware complexity of digital receive beamformers, beamforming techniques based on sigma-delta ($\Sigma\Delta$) ADC were proposed [3], [4]. In a sigma-delta beamforming (SDBF) system, the multi-bit ADCs are replaced with sigma-delta ADCs. Because the sigma-delta ADC typically uses a single-bit quantizer running at high frequency, the beamformer does not require computationally expensive interpolation or a phase rotation unit to provide the necessary delay accuracy [5]. Compared with other types of ADCs (e.g., flash, folding), sigma-delta ADCs are also more robust against circuit imperfections [6]. Another important advantage is that SDBF has the potential to be integrated into a single chip, eliminating the expensive interconnection and packaging [4], [7].

By directly replacing the multi-bit ADCs with sigma-delta ADCs of similar resolution (including modulators and reconstruction filters), the (pre-delay reconstruction) SDBF can provide comparable image quality to the conventional multi-bit beamformer. However, the hardware is still complex due to the use of a computationally demanding reconstruction filter in each channel. To alleviate the hardware requirement in the pre-delay reconstruction SDBF, Noujaim *et al.* developed a post-delay reconstruction SDBF [3] in which one reconstruction filter is used after the delay-and-sum process (instead of one filter in each channel) to recover the modulated signal. This approach significantly reduces the hardware but it suffers from dynamic focusing artifacts that are introduced when samples are repeated during the delay-and-sum process.

To reduce dynamic focusing artifacts in post-delay reconstruction SDBF, several methods have been proposed. Freeman *et al.* presented 2 digital processing techniques: the insert-zero and divide-by-2 methods [4], [8]. The insert-zero method replaces the repeated samples with zeros, whereas the divide-by-2 method reduces the sample to half before it is repeated. Due to the additional zero level needed, the insert zero method involves bit growth during beam-summation. Hence, based on the insert zero method, Rigby and Li *et al.* proposed insert $+1$, -1 [9] and symmetrical hold [10] methods, respectively, to avoid the bit growth. The contrast resolution that these methods can provide is still limited, especially when delay update is dynamic (at near field). Han *et al.* also developed a multiplier-less pre-delay reconstruction SDBF that is free from dynamic focusing artifacts [11], [12]. However, the pre-delay reconstruction filter, which consists of multiple multi-bit accumulators and a filter coefficient look-up-

Fig. 1. Point phantom images: (a) without dynamic focusing artifacts and (b) with dynamic focusing artifacts.

table (LUT) in each channel, still contributes to a large amount of hardware.

Section II of this paper shows that, to achieve a similar image quality as pre-delay reconstruction SDBF, it is not necessary to have a complex pre-delay reconstruction filter in each channel. Based on the findings in Section II, Section III describes a new cascaded reconstruction SDBF that uses simple boxcar filters as the pre-delay filters. Section IV explains the selection of filters in the developed beamformer to optimize the beamformer performance, and Section V presents simulation results and discussions on the overall system.

II. Dynamic Focusing Artifacts

Due to the high sampling frequency of SDBF, sufficient delay resolution can be achieved directly with the delay-and-sum approach. The delay-and-sum beamforming method selects a sample in each channel according to the quantized delay profile. A dynamic delay is realized by repeating a sample. However, in SDBF, when sigma-delta modulator output samples are repeated, the signal cannot be reconstructed properly and artifacts will be introduced in the final image. This effect is shown in Fig. 1 where Fig. 1(a) and 1(b) show point phantom images (in 60 dB dynamic range when a dynamic aperture is applied at f-number ≥ 2) with and without dynamic focusing artifacts, respectively. As indicated in Fig. 1(b), dynamic focusing artifacts cause background noise in the image, resulting in severe reduction of the image contrast resolution.

A. Time Domain Analysis

The sample repetition inserts extra noise that is not properly shaped by the noise-shaping function. A set of simulations was carried out to study the effect of quantization noise on dynamic focusing artifacts, and the results are shown in Fig. 2. In these simulations, a radio frequency (RF) signal consisting of a 0.6 fractional bandwidth and a 3.5 MHz Gaussian pulse with −50 dB white noise was used. The RF signal was digitized at 111 MHz using a single-bit 2nd-order low-pass sigma-delta modulator, and reconstruction was done using a 160-tap low-pass FIR filter to achieve a 2 MHz transition band (4 MHz to 6 MHz), 0.01 dB peak passband ripple, and 50 dB minimum stopband attenuation. A higher order sigma-delta modulator provides better bit resolution, but a 2nd-order sigma-delta modulator was used because any single bit sigma-delta modulator higher than 2nd order is not inherently stable [13].

Fig. 2(a) shows the normalized waveform of the RF signal after it goes through sigma-delta modulation, reconstruction, single sample repetition (every 50 sample interval), and then envelope detection in sequence. On the other hand, Fig. 2(b) shows the normalized waveform of the RF signal after it goes through the sequence of sigma-

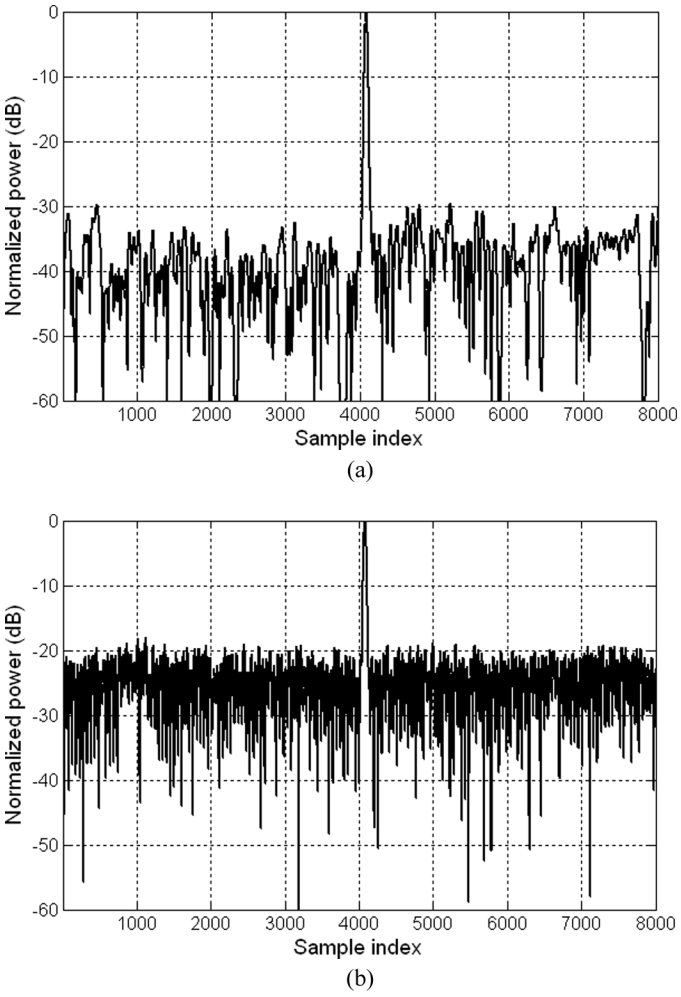

Fig. 2. RF signal waveform after going through (a) sigma-delta modulation, reconstruction, sample repetition, and envelope detection in sequence and (b) sigma-delta modulation, sample repetition, reconstruction, and envelope detection in sequence.

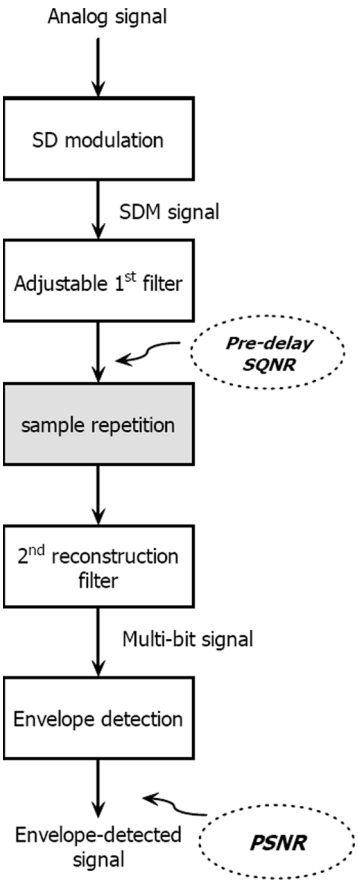

Fig. 3. Simulation setup that investigates the effect of pre-delay SQNR on PSNR.

delta modulation, single sample repetition (at 50-sample intervals), reconstruction, and envelope detection.

The peak signal-to-noise ratio (PSNR) of the 2 cases can be obtained from the results in Fig. 2 as the ratio of the peak signal power to the average noise floor level [14]. The ratio is calculated based on the assumption that the signal distortion (noise floor) is low compared with the signal power. The PSNR of the 2 cases are, respectively, 45 dB and 28 dB for an average of 5 runs. It demonstrates that sample repetition before signal reconstruction increases the noise floor of the final output.

An additional 160-tap low pass FIR filter was inserted into the simulation setup as the adjustable 1st filter shown in Fig. 3 to vary the quantization noise level before sample repetition and to study the effect of sample repetition at different pre-delay quantization noise levels.

The signal now goes through sigma-delta modulation, adjustable 1st filter, sample repetition, 2nd reconstruction filter, and then envelope detection. By adjusting the out-of-band attenuation of the 1st filter, a pre-delay signal with different quantization noise levels can be obtained. The PSNR value of the envelope-detected signal after 2nd reconstruction filter was plotted against the pre-delay signal-to-quantization noise ratio (SQNR) of the signal after 1st filter, as shown in Fig. 4. Because, in practice, the sample repetition rate is dynamically changing along the

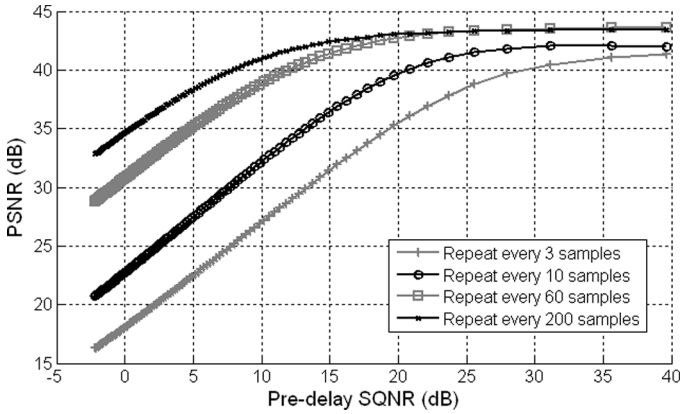

Fig. 4. Single channel PSNR obtained against different pre-delay SQNR at different sample repetition rate.

imaging depth, the simulation was repeated for different sample repetition rates.

As shown in Fig. 4, when the sample repetition is less frequent, PSNR is higher. In addition, as the pre-delay SQNR increases, the PSNR achieved at that channel after sample repetition increases as well. It shows that the pre-delay quantization noise level affects the degree of dynamic focusing artifacts. The lower the quantization noise level, the lower the dynamic artifacts caused by sample repetition. Fig. 4 also shows that when the pre-delay SQNR is high, the increment of PSNR with respect to pre-delay SQNR will become gradual, and testing additional increments of the pre-delay SQNR will not make much improvement on the PSNR. It is therefore not necessary to reconstruct the signal fully before the delay-and-sum process; a partial reconstruction is sufficient.

B. Frequency Domain Analysis

Another frequency domain simulation was carried out to study the effect of dynamic focusing on the spectrum of sigma-delta modulated signals. A similar simulation setup as shown in Fig. 3 was used. The only difference is that the samples were repeated dynamically to model the delay profile at the outermost channel of a 64-channel beamformer.

The input signal is a pre-compressed waveform, which when properly delayed according to the dynamic delay profile will be a single tone sinusoidal wave at 3.5 MHz. The input signal was digitized using a 2nd-order low-pass sigma-delta modulator at 160 MHz. The frequency spectra of the sigma-delta modulated signal before and after the dynamic delay without applying any pre-delay filtering are shown in Fig. 5(a). When an 8-tap boxcar filter is used as the pre-delay filter, the frequency spectra of the signal before and after the dynamic delay are as shown in Fig. 5(b).

As depicted in Fig. 5(a), besides the compression and shifting of the signal frequency, the noise power at low frequency increases significantly, and no noise shaping function is observed after dynamic delay is applied. The low frequency noise causes image artifacts because it cannot

be removed by the low-pass reconstruction filter. On the other hand, when an 8-tap boxcar filter is used before delay, the noise level caused by dynamic delay is 20 dB lower compared with the previous case without any pre-delay filtering. The frequency domain analysis again justifies the hypothesis that reducing pre-delay quantization noise can alleviate the dynamic focusing artifacts.

Based on the findings, we proposed and developed a SDBF based on cascaded reconstruction, which reduces the pre-delay quantization noise to suppress the dynamic focusing artifacts.

III. Cascaded Reconstruction Sigma-Delta Beamforming

A cascaded reconstruction process for sigma-delta modulation is shown in Fig. 6. The reconstruction of the sigma-delta modulated signal is performed by 2 filters. The first filter in Fig. 6 is a computationally inexpensive filter to partially reconstruct the signal, whereas the second filter fully reconstructs the complete multi-bit signal. Both first and second filters can be composed of a single stage filter or a set of cascaded filters, as long as they provide the necessary filtering effect.

The cascaded reconstruction is employed in the developed SDBF, in which the first filter is applied before dynamic focusing and the second filter is applied after the delay-and-sum process, as illustrated in Fig. 7.

The analog signal from each receive channel is digitized with a sigma-delta modulator, and then the first filter is applied to partially reconstruct the intermediate multi-bit data from the single bit modulator output data. Unlike the sophisticated filters used in the pre-delay reconstruction SDBF to fully reconstruct the signal, this first filter can be realized using a computationally inexpensive filter (e.g., boxcar or cascaded integrator comb [CIC]), provided that it achieves the required pre-delay SQNR as discussed in Section II. Therefore, the hardware complexity can be reduced while achieving a significant reduction in dynamic focusing artifacts. Moreover, with the lower SQNR value required, the intermediate multi-bit data can have a lower bit depth than the fully reconstructed data (after 2nd filter). The intermediate multi-bit data generated at each channel is then temporarily stored in a multi-bit shift register or first-in-first-out (FIFO) memory. After that, focusing delay for each beamforming output is applied to select the appropriate intermediate multi-bit sample from each channel. This focusing delay can either be pre-computed and stored in an LUT or calculated in real time. The selected intermediate multi-bit data are then summed across the channels to improve spatial and contrast resolution by coherent summation. After the delay-and-sum process, the second filter is applied to fully reconstruct the complete multi-bit data for back-end processing.

To reduce the hardware complexity further in the temporary storage devices (e.g., shift register or FIFO memory), the sequence of the first filter and delay focusing can

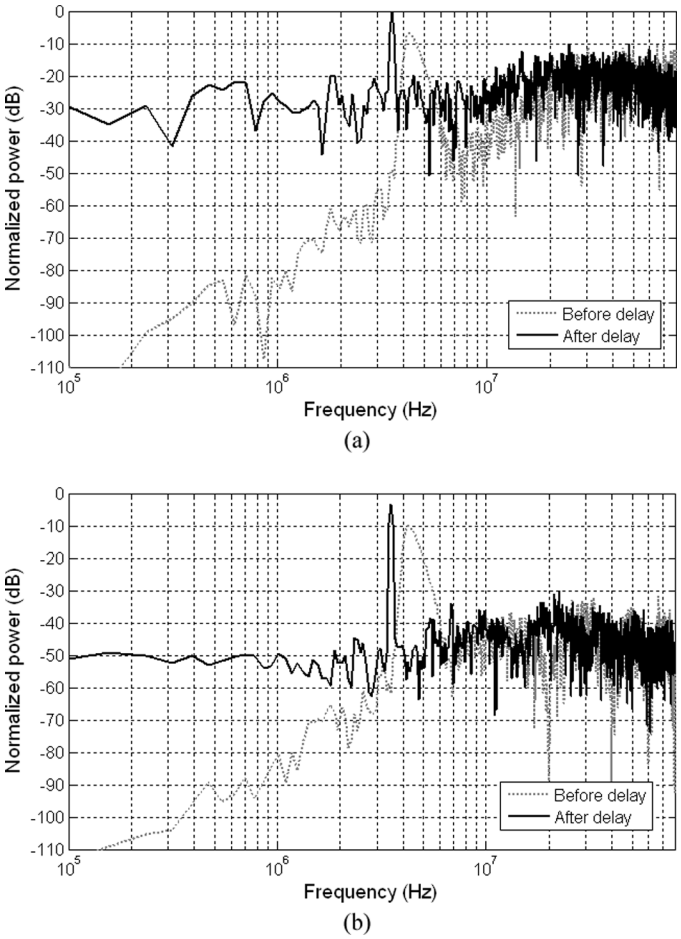

Fig. 5. Frequency spectra of sigma-delta modulated signal before and after dynamic delay when (a) no pre-delay filtering is used and (b) when an 8-tap boxcar filter was used as pre-delay filter.

be interchanged. This is explained in Fig. 8 where 4-tap filtering and delay focusing stages are shown.

As shown in Fig. 8(a), a 4-tap filter with coefficients of $C_1 \sim C_4$ is applied on a stream of 1-bit samples, S_1, S_2, S_3 ... S_N to generate M-bit output samples, S'_1, S'_2, S'_3 ... S'_{N-3}. Each output sample is the sum of the products of 4 consecutive input samples with the corresponding filter coefficients. During the delay focusing stage, one of the output samples is selected according to the delay information. If S'_1 is selected, it is equivalent to selecting the sum of $S_1 \times C_4$, $S_2 \times C_3$, $S_3 \times C_2$ and $S_4 \times C_1$. Therefore, the same beamforming result can be attained by selecting the 4 samples S_1, S_2, S_3, S_4 before multiplying with the filter coefficients and summation as shown in Fig. 8(b). As a result, instead of storing the M-bit data, single-bit data are stored in the temporary storage devices, waiting to be selected during delay focusing, thereby optimizing the hardware.

Fig. 9 shows the block diagram of the cascaded reconstruction SDBF where delay focusing is performed before the first reconstruction filtering.

At each instant, K consecutive single-bit input samples are selected by the delay control from the shift register (or FIFO memory), where K is equal to the length of the first filter. They are then multiplied with the filter coefficients

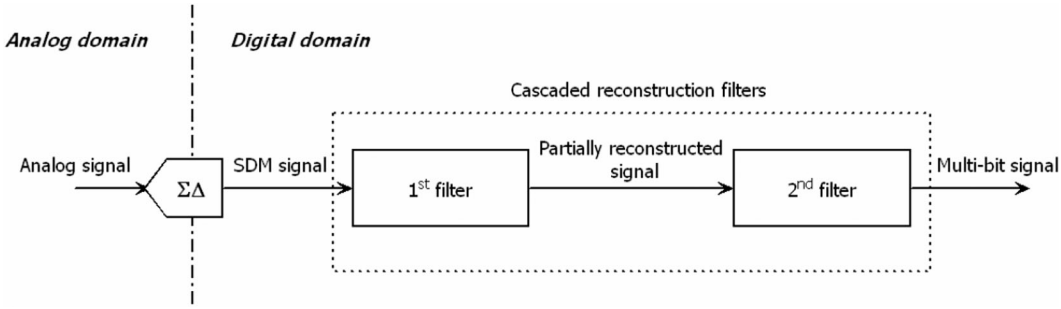

Fig. 6. Cascaded reconstruction of a sigma-delta modulated bit stream.

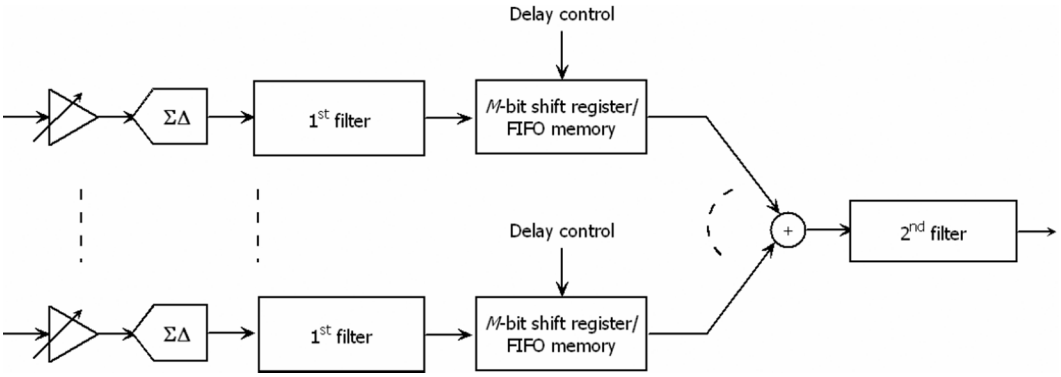

Fig. 7. Block diagram of an SDBF based on cascaded reconstruction.

and summed together along the same channel to obtain the intermediate multi-bit data. To eliminate computationally expensive multipliers from the beamformer, boxcar filters can be used as the first filters. This will further simplify the hardware.

IV. First Filter Selection

As mentioned previously, boxcar filters can be utilized as the first filters to minimize the hardware complexity. It is desirable to select the boxcar filters to be as simple as possible while achieving the required image quality. Section II illustrated that different pre-delay SQNR are needed before the delay-and-sum process to achieve the required PSNR at different sample repetition rate. In practice, the sample repetition rate is limited because the dynamic aperture is usually employed to optimize focusing at different depths. The maximum sample repetition rate caused by dynamic focusing was found to be related to the *f*-number (which is defined as the ratio of focal length to the aperture size [15]) only. *F*-number of 2 will be used in the following illustration. The maximum sample repetition rate can be obtained using the time difference, Δt_n, between 2 consecutive time of arrival, t_{n1} and t_{n2}, assuming that the aperture size is small compared with the focal depth [4],

$$t_{n1} \approx \frac{R}{c} + \frac{\left(R - x_n \sin\theta + \dfrac{x_n^2 \cos^2\theta}{2R}\right)}{c}, \tag{1}$$

$$t_{n2} \approx \frac{R + \Delta R}{c} + \frac{\left(R + \Delta R - x_n \sin\theta + \frac{x_n^2 \cos^2\theta}{2(R+\Delta R)}\right)}{c}, \tag{2}$$

$$\Delta t_n \approx T\left(1 - \frac{x_n^2 \cos^2\theta}{4} \frac{1}{R(R+\Delta R)}\right), \tag{3}$$

where R is the focal depth, c is the speed of sound, x_n is the distance between the nth element to the center of the active transducer aperture, θ is the steering angle, T is the sampling period that is equal to $\Delta R/2c$. When R is much larger than ΔR, the minimum time difference is

$$\Delta t_{n\min} \approx T\left(1 - \frac{x_{n\max}^2}{4}\frac{1}{R^2}\right) = T\left(1 - \frac{1}{16 f_{\text{num}}^2}\right), \tag{4}$$

where *f*-number is equal to $R/2x_{n\,\max}$.

The minimum number of sample interval, $p_{\min}$, between 2 occurrences of sample repetition can be calculated as

$$p_{\min} = \frac{T}{T - \Delta t} = 16 f_{\text{num}}^2, \tag{5}$$

Hence, when *f*-number is 2, samples will be repeated at the maximum rate of every 64 samples.

The required pre-delay SQNR and achievable PSNR (per channel) when samples are repeated every 64 samples were obtained by repeating the simulations described in Section II at a different oversampling ratio (OSR, which is defined as $f_S/2f_B$, where f_S is the sampling frequency and f_B is the signal bandwidth). The same RF signal, which

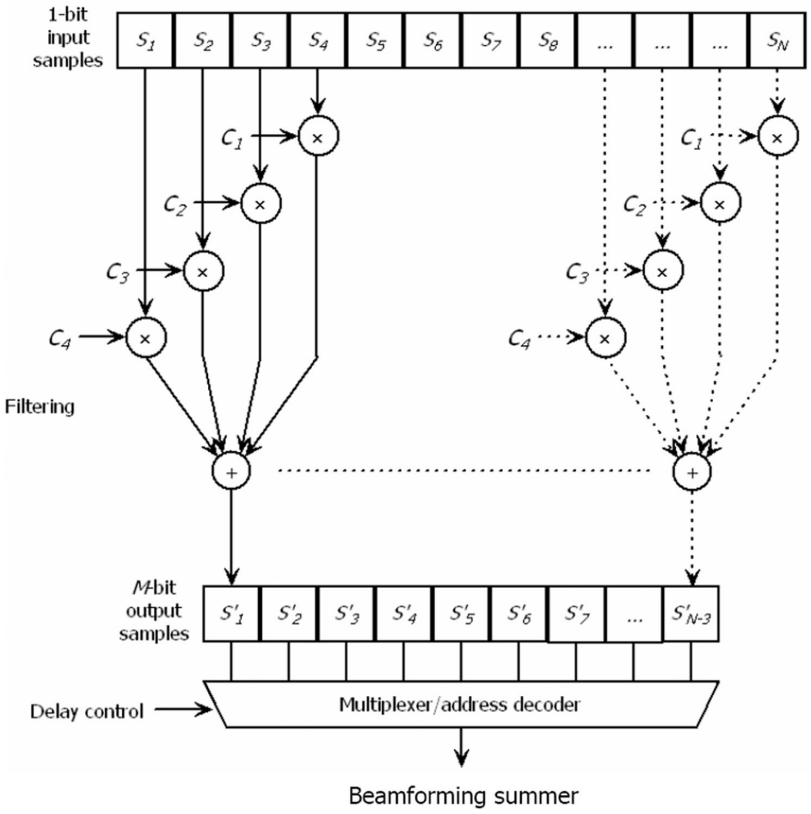

Fig. 8. Block diagram showing the difference in hardware requirement by applying delay focusing (a) after the first filter and (b) before the first filter.

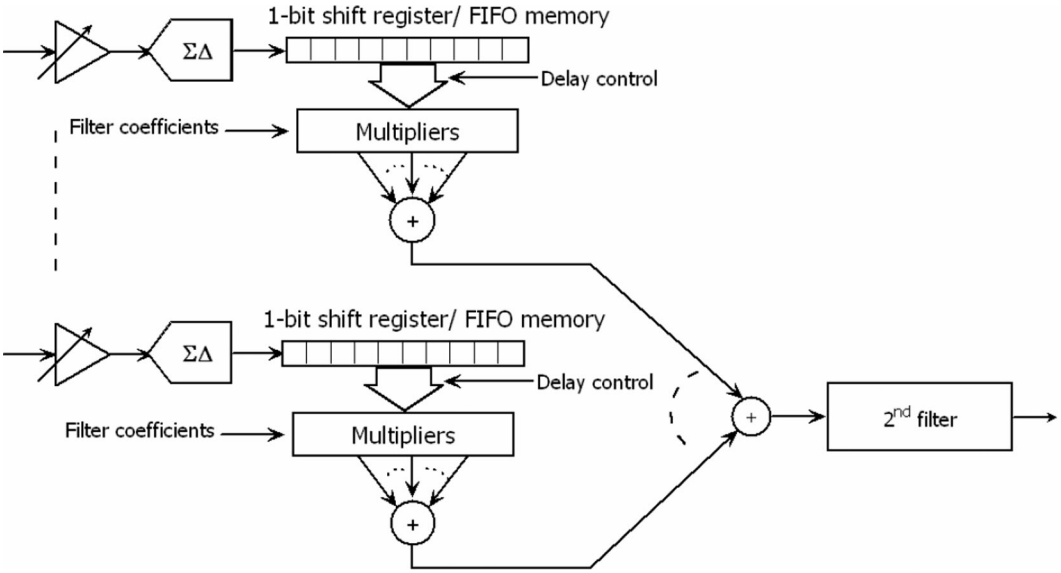

Fig. 9. Cascaded reconstruction SDBF where delay focusing is performed before the first filtering.

consists of a 0.6 fractional bandwidth, 3.5 MHz Gaussian pulse was used. White noise was inserted at a level 10 dB lower than the theoretical dynamic range (DR) of a 2nd-order sigma-delta modulator, which can be calculated using

$$\mathrm{DR} = \frac{15(\mathrm{OSR})^5}{2\pi^4}, \tag{6}$$

assuming the input as a sine wave with amplitude of 1 [13].

The average maximum PSNR and the −3 dB corner SQNR (at which the PSNR achieved is −3 dB below the maximum value) for 10 runs of the repeat-every-64-sample simulation are plotted against the OSR as in Fig. 10. They are denoted as the achievable PSNR and required pre-delay SQNR. As the noise floor of the normalized envelope-detected RF signal is dominated by the quantization noise of the modulator output, the PSNR will be equal to the SQNR of the modulator output, which is also the dynamic range (DR) of the modulator.

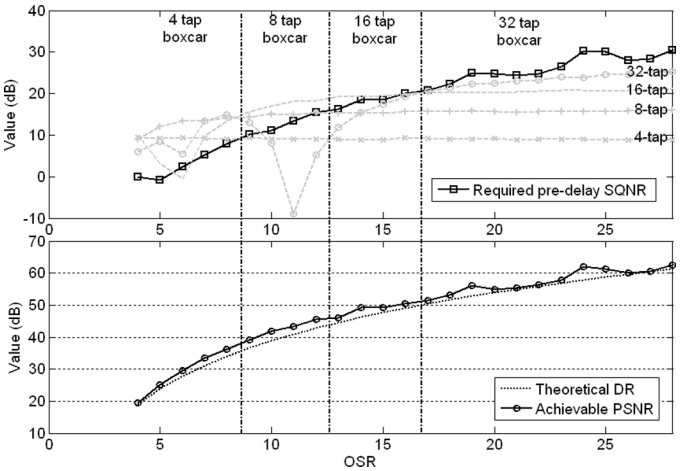

Fig. 10. Required pre-delay SQNR at different OSR and the corresponding achievable PSNR per channel after beamforming.

The same simulation was carried out using the setup in Fig. 3 under the same condition but with the 1st adjustable filter replaced by 4-tap, 8-tap, 16-tap, and 32-tap boxcar filters to find the suitable OSR range for each of them to be applied. The pre-delay SQNR achieved by different filters under different OSR are plotted as the dotted lines in the upper graph of Fig. 10 as well.

Fig. 10 shows that when OSR is below 9, a 4-tap boxcar filter is sufficient to provide the required pre-delay SQNR for the beamformer to achieve −3 dB PSNR value. The pre-delay SQNR achieved by a 32-tap boxcar filter shows 2 notches at OSR of 6 and 11 because the signal falls into the notches of the boxcar filter's frequency response, which is at the multiples of fs/tapsize. It should be noted that for OSR above 17, a 32-tap boxcar filter does not really meet the −3 dB corner SQNR requirement. Hence, to obtain a better performance, a more sophisticated filter needs to be used. However, if a boxcar filter is to be used for its hardware advantage, 32-tap size is the best candidate.

Fig. 10 provides the condition for the selection of OSR and boxcar filter length. For example, if a 40 dB DR per channel is required for a SDBF, the sigma-delta modulator in each channel needs to run at an OSR of 11. The pre-delay SQNR has to be higher than 14 dB to sufficiently suppress the dynamic focusing artifacts. Thus, an 8-tap boxcar filter is sufficient to achieve the required pre-delay SQNR.

V. Results and Discussions

The developed cascaded reconstruction SDBF was evaluated using the data acquired by Biomedical Ultrasonics Laboratory at the University of Michigan (available at http://bul.eecs.umich.edu). The data were collected using

Acuson, Model #V328, a 128-element, 3.5 MHz commercial transducer for a wire target phantom consisting of 6 wires in a water tank (Acuson Mountain View, CA). The same data were also used for comparison by [4] and [10].

To achieve a maximum average sidelobe level of −30 dB for both transmission and reception (for a 128-channel array with rectangular windowing), the sampling frequency required to achieve sufficient delay resolution can be calculated using the peak random quantization sidelobe (voltage) level equation in [16]

$$\mathrm{SL}_{\mathrm{peak}} \approx \frac{\pi}{m}\left(\frac{4.6\mathrm{ENBW}}{3N}\right)^{\frac{1}{2}}, \tag{7}$$

where ENBW is the equivalent noise bandwidth, which is 1 in this case when a rectangular window is used for apodization; m is the ratio of sampling frequency to signal frequency, which is equal to 2 × OSR; and N is the number of elements, under the condition that the error components are uncorrelated from channel to channel. The condition of random noise (uncorrelated with signal, hence uncorrelated among channels) is true for sigma-delta modulation when the modulator has an active input [17], which is true for the case of ultrasound imaging.

From (7), m is found to be 11 for the system described. Hence, the sampling frequency needs to be at least 11 times higher than the central frequency of the ultrasound signal (for a 128-channel array with rectangular windowing), equivalent to an OSR of 5.5. For 64 channels, it would be 16 times higher, and for 32 channels, it would be 22 times higher.

On the other hand, the sampling frequency of a sigma-delta beamformer also determines the DR that can be achieved for the final image. For a 128-channel array with rectangular windowing, the apodization power gain is

$$G_{\mathrm{SNR}} = \frac{\left(\sum_{n=1}^{N} w_n\right)^2}{\sum_{n=1}^{N} w_n^2} = 21 \text{ dB}, \tag{8}$$

where w_n is the weighting of the nth channel. To obtain a total DR of 60 dB, the DR needed for each channel is 39 dB.

For a single-bit 2nd-order sigma-delta modulator, the OSR needed can be estimated using (6). Alternatively, the equation can be expressed in terms of dB as

$$\mathrm{DR} = 1.76 - 12.9 + 50 \log \mathrm{OSR}\ (\mathrm{dB}). \tag{9}$$

OSR was found to be 10.1 to obtain a DR of 39 dB. That means the sampling frequency needs to be at least 20.2 times higher than the signal bandwidth. An OSR of 11 can be selected to fulfill the DR requirement for a low-resolution hand-held machine. The DR achieved would be 41 dB. Hence, for the following simulations, the wire phantom data were converted into 1-bit data streams using typical single-bit 2nd-order low-pass sigma-delta modulators at a sampling frequency of 111 MHz (OSR of 11 for 5 MHz bandwidth). Nevertheless, higher OSR can be used to ensure that the quantization noise is well below input noise level and electronic noise for a higher resolution machine.

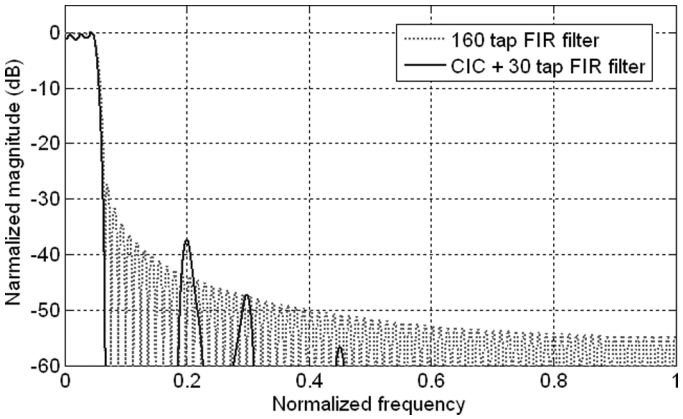

Fig. 11. Frequency responses of 160 tap FIR filter and CIC decimator with 30 tap FIR filter.

From Fig. 10, an 8-tap boxcar filter was chosen as the first filter to provide the required pre-delay SQNR. Three different SDBF techniques (i.e., pre-delay reconstruction, post-delay reconstruction, and insert-zero) were compared with the developed method. A 160-tap FIR filter was used in the pre-delay reconstruction method. Post-delay reconstruction for all techniques was performed with a 3rd-order cascaded integrator-comb (CIC) decimation filter followed by a 30-tap FIR filter. The 160-tap FIR filter and the CIC decimator cascaded with a 30-tap FIR filter can achieve a similar pass-band filter characteristic as shown in Fig. 11, thus providing a fair image quality comparison and practical hardware comparison.

The images obtained with dynamic aperture at *f*-number ≥ 2 are shown in Fig. 12 with 60 dB dynamic range. Axial projection was plotted alongside to show the different noise levels, which cannot be visually differentiated from the images.

As shown in Fig. 12, the post-delay reconstruction method, i.e., Fig. 12(b), suffers from noisy image background due to dynamic focusing artifacts, whereas the other methods, including the developed cascaded reconstruction, have cleaner image background. Comparing Fig. 12(c) and 12(d), the cascaded reconstruction SDBF produces less background noise than the insert zero method, as supported by the axial projection.

PSNR was calculated from the images based on the ratio of the peak signal power of the images, which is at the 3rd wire target from top in Fig. 13, to the average background noise within the 3 boxed areas as indicated in Fig. 13. The results obtained for different beamforming techniques are shown in Table I.

Table I shows that, at 111 MHz, cascaded reconstruction SDBF is able to achieve better contrast resolution

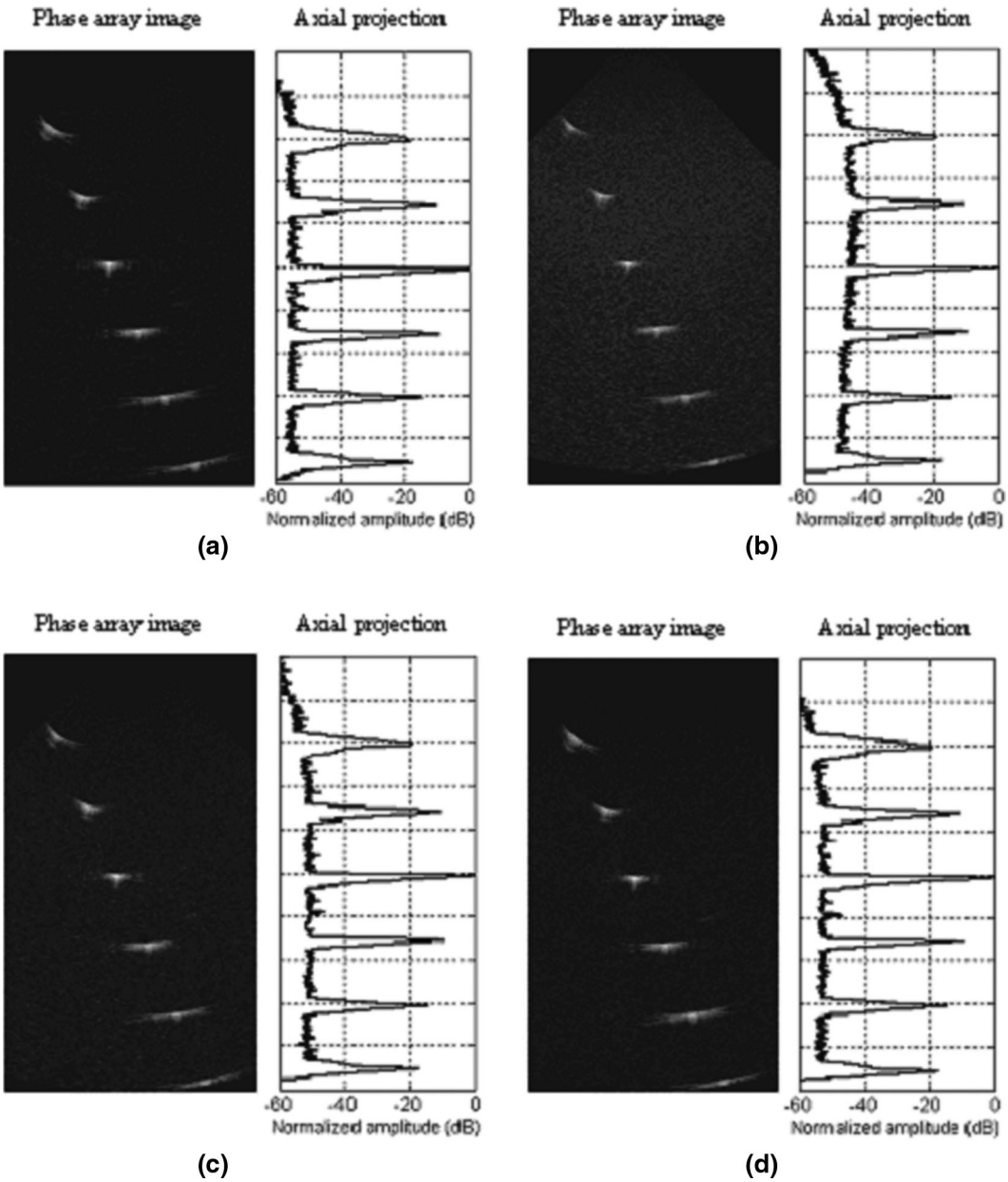

Fig. 12. Wire phantom images with axial projection obtained using (a) pre-delay reconstruction, (b) post-delay reconstruction, (c) insert zero, and (d) cascaded reconstruction SDBF.

than insert zero method. Boxcar filters have notches in their frequency response at frequencies that are the multiples of f_S/tapsize. For example, a 4-tap boxcar filter has notches at $f_S/4$, $f_S/2$, $3f_S/4$, and f_S . When the tap size increases, the number of notches in the frequency response will increase and more out-of-band quantization noise can be filtered off. Hence, using a 16-tap boxcar filter as the 1st filter can achieve higher PSNR than using an 8-tap boxcar filter and 4-tap boxcar filter. However, the tap size of the boxcar filter should not be further increased to the extent that it attenuates the signal whose bandwidth is at $f_S/22$ in this case (OSR = 11). Table I also shows that, when using an 8-tap boxcar filter as the 1st filter, the PSNR achieved will be within the −3 dB range from that achieved by the pre-delay reconstruction method.

Another set of cyst phantom data acquired by Biomedical Ultrasonics Laboratory at the University of Michigan was used to evaluate the proposed cascaded reconstruction SDBF (using an 8-tap boxcar filter as the 1st filter) against the same 3 methods. This same set of data was also used for comparison by [4] and [10]. The image formed by the data is shown in Fig. 14. The contrast resolution achieved by the different methods was evaluated in terms of contrast-to-noise ratio (CNR).

CNR is defined as

$$\mathrm{CNR} = \frac{|\,\mu_s - \mu_c\,|}{\sigma_s}, \tag{10}$$

where μ_s and μ_c denote the mean values of the scatterers and of the cyst, respectively, and σ_s is the standard devia-

TABLE I. PSNR VALUES OF 3 DIFFERENT DEPTHS FOR DIFFERENT BEAMFORMING TECHNIQUES AT 111 MHz BEAMFORMING FREQUENCY.

		PSNR 1(dB)	PSNR 2(dB)	PSNR 3(dB)
Pre-delay reconstruction		62.68	62.56	62.62
Post-delay reconstruction		51.74	54.48	55.68
Insert zero		58.79	58.55	58.76
Cascaded reconstruction using different 1st filters	4-tap boxcar	59.09	59.21	59.50
	8-tap boxcar	60.77	60.53	60.79
	16-tap boxcar	62.17	62.11	62.07

TABLE II. CONTRAST-TO-NOISE RATIO (CNR) IN ANECHOIC REGION OF THE CYST PHANTOM IMAGE OBTAINED BY VARIOUS SDBF.

Cyst	Pre-delay reconstruction	Post-delay reconstruction	Insert zero	Cascaded reconstruction
1 (50 mm)	6.19	5.07	5.95	6.15
2 (80 mm)	6.14	5.30	5.88	6.01
3 (110 mm)	4.35	3.55	4.07	4.30

tion of the scatterers [18]. The results of the CNR for 60 dB dynamic range are presented in Table II.

The results in Table II again indicate that the proposed cascaded reconstruction SDBF is able to provide better contrast resolution than the insert zero method, and the performance is very close to pre-delay reconstruction SDBF.

The hardware of the proposed cascaded reconstruction SDBF can be greatly simplified compared with pre-delay reconstruction method by using a much simpler pre-delay filter in each channel, and this is demonstrated in Table III, which presents the hardware comparison between pre-delay reconstruction and cascaded reconstruction (using an 8-tap boxcar filter as the 1st filter) methods for a 64-channel beamformer. The number of multipliers needed can be reduced from 5120 (80 per channel as the filter coefficients are symmetric) to 15 (for the 30-tap FIR filter after CIC decimator), and the adders can be reduced from 10 240 (160 per channel) multi-bit adders to 64 (1 per channel) 8-input-single-bit adders and 36 multi-bit adders (for a 3rd-order CIC decimator and 30-tap FIR filter).

VI. CONCLUSIONS

Post-delay reconstruction SDBF suffers from artifact problems when dynamic focusing is performed. It was found that the artifact problem is related to the quantization noise present in the sigma-delta modulated signal. The relationship between the image quality (in terms of PSNR) and the quantization noise before sample repetition is studied in this paper. The study shows that dynamic focusing artifacts can be effectively suppressed when a certain SQNR is achieved for the signal before the delay focusing. Hence, we proposed and developed a cascaded reconstruction SDBF that effectively suppresses the dy-

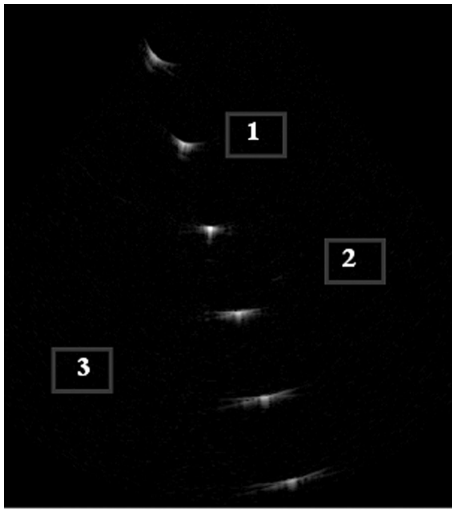

Fig. 13. Wire phantom image that shows the 3 areas of noise power that are used to calculate the PSNR.

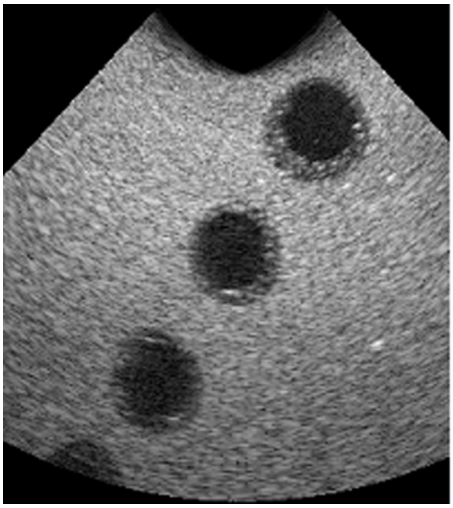

Fig. 14. Image of the cyst phantom data acquired by Biomedical Ultrasonics Laboratory at University of Michigan.

TABLE III. NUMBER OF MULTIPLIERS AND ADDERS FOR PRE-DELAY RECONSTRUCTION SDBF AND CASCADED RECONSTRUCTION SDBF WITH 8-TAP BOXCAR PRE-DELAY FILTER FOR 64-CHANNEL SYSTEM.

Pre-delay reconstruction		Cascaded reconstruction	
Components	Number	Components	Number
Pre-delay reconstruction filter			
Multi-bit multipliers	80 × 64 ch = 5120	8-input 1-bit adder	1 × 64 ch = 64
Multi-bit adders	160 × 64 ch = 10240		
Post-delay reconstruction filter			
		Multi-bit multipliers	15
		Multi-bit adders	36
Beamforming summer			
64-input 8-bit adder	1	64-input 4-bit adder	1

namic focusing artifacts by reducing the pre-delay quantization noise using boxcar filters.

This paper also presents the conditions to select the tap size of boxcar filters for different OSR when a dynamic aperture is applied at *f*-number of 2. Simulation results using real phantom data show that the dynamic focusing artifacts can be reduced by simply using an 8-tap boxcar filter as the pre-delay filter when OSR is 11. The contrast resolution of the image produced by the proposed SDBF is comparable to that produced by the pre-delay reconstruction beamforming method and is better than that of the insert zero method. The hardware can also be greatly simplified compared with pre-delay reconstruction method due to the much simpler filter used in each channel.

ACKNOWLEDGMENTS

The authors would like to thank Y. M. Yoo, A. Agarwal, F. K. Schneider, and Y. Kim from Image Computing Systems Laboratory, Department of Electrical Engineering, at Bioengineering University of Washington for their valuable advice at different stages of the research.

REFERENCES

[1] V. S. Gierenz, R. Schwann, and T. G. Noll, "A low power digital beamformer for handheld ultrasound systems," in *Proc. 27th European Solid-State Circuits Conference*, 2001, pp. 261–264.

[2] R. Mucci, "A comparison of efficient beamforming algorithms," *IEEE Trans. Acoust. Speech Signal Process.*, vol. 32, no. 3, pp. 548–558, 1984.

[3] S. E. Noujaim, S. L. Garverick, and M. O'Donnell, "Phased array ultrasonic beam forming using oversampled A/D converters," U. S. Patent 5203335, April 20, 1993.

[4] S. R. Freeman, M. K. Quick, M. A. Morin, R. C. Anderson, C. S. Desilets, T. E. Linnenbrink, and M. O'Donnell, "Delta-sigma oversampled ultrasound beamformer with dynamic delays," *IEEE Trans. Ultrason. Ferroelectr. Freq. Control*, vol. 46, no. 2, pp. 320–332, Mar. 1999.

[5] M. Inerfield, G. R. Lockwood, and S. L. Garverick, "A sigma-delta-based sparse synthetic aperture beamformer for real-time 3-D ultrasound," *IEEE Trans. Ultrason. Ferroelectr. Freq. Control*, vol. 49, no. 2, pp. 243–254, 2002.

[6] M. Karaman and M. Kozak, "An asynchronous oversampling beamformer," WIPO PCT, Patent Appl. PCT/TR98/00019, Aug. 24, 1998.

[7] B. G. Tomov and J. A. Jensen, "Compact FPGA-based beamformer using oversampled 1-bit A/D converters," *IEEE Trans. Ultrason. Ferroelectr. Freq. Control*, vol. 52, no. 5, pp. 870–880, 2005.

[8] S. R. Freeman, M. O'Donnell, T. E. Linnenbrink, M. A. Morin, M. K. Quick, and C. S. Desilets, "Beamformed ultrasonic imager with delta-sigma feedback control," U. S. Patent 5964708, Oct. 12, 1999.

[9] K. W. Rigby, "Delta-sigma beamformers with minimal dynamic focusing artifacts," U. S. Patent 6366227 B1, Apr. 2, 2002.

[10] P.-C. Li, J.-J. Huang, H.-L. Liu, and M. O'Donnell, "A dynamic focusing technique for delta-sigma based beamformers," *Ultrason. Imag.*, vol. 22, pp. 197–205, 2000.

[11] H.-S. Han and T.-K. Song, "Multiplierless sigma-delta modulation beam forming for ultrasound nondestructive testing," *Key Eng. Mater.*, vol. 270–273, pp. 215–220, May. 2004.

[12] H.-S. Han, T.-S. Song, B.-H. Kim, and H.-H. Kim, "Error-free pulse compression method for ultrasound beamforming using sigma-delta modulation," in *Proc. IEEE Ultrason. Symp.*, 2006, pp. 2140–2143.

[13] R. Schreier and G. C. Temes, *Understanding Delta-Sigma Data Converters*. Piscataway/Hoboken/Chichester, NJ: Wiley, 2005.

[14] S. I. Nikolov and J. A. Jensen, "Comparison between different encoding schemes for synthetic aperture imaging," Proc. SPIE Medical Imaging Meeting, Ultrasound Imaging and Signal Processing, 2002.

[15] W. R. Hedrick, D. L. Hykes, and D. E. Starchman, *Ultrasound Physics and Instrumentation*, 3rd ed., St. Louis, MO: Mosby, Inc., 1995.

[16] S. Holm and K. Kristoffersen, "Analysis of worst-case phase quantization sidelobes in focused beamforming," *IEEE Trans. Ultrason. Ferroelectr. Freq. Control*, vol. 39, no. 5, pp. 593–599, 1992.

[17] J. Candy and O. Benjamin, "The structure of quantization noise from sigma-delta modulation," *IEEE Trans. Commun.*, vol. 29, no. 9, pp. 1316–1323, 1981.

[18] M. Karaman, P.-C. Li, and M. O'Donnell, "Synthetic aperture imaging for small scale systems," *IEEE Trans. Ultrason. Ferroelectr. Freq. Control*, vol. 42, no. 3, pp. 429–442, 1995.

Jia Hao Cheong was born in Johor, Malaysia, in 1982. He received his B.Eng. degree in electrical and electronic engineering from Nanyang Technological University (NTU), Singapore, in 2005.

In April 2005, he was offered a research scholarship by NTU, where he is currently pursuing his Ph.D. degree. His research interests include oversampled ultrasound beamforming, analog/mixed signal and digital IC design, and ultra-wideband transceiver design.

He was awarded the Panasonic Gold Medal and Motorola Book Prize for being the best student with the highest aggregate marks in IC design specialization and the best student in the course VLSI Circuits & Systems, respectively, during his B.Eng. study.

Yvonne Ying Hung Lam received her B.Sc. degree from the Aston University in Birmingham (UK) in 1982 and both her M.Sc. and Ph.D. degrees from the University of Southampton (UK) in 1989 and 2001, respectively. Her Ph.D. research was on the topic of analog circuit synthesizer.

From 1982 to 1983, she worked as an engineer in Telecommunication Authority of Singapore (TAS). From 1984 to 1987, she worked first as a CAD engineer, then as an IC designer for consumer market with SGS (now known as ST-Microelectronics) Agrate-, Castelletto-Milano (Italy), and Asia Pacific Design Center (Singapore). She joined Nanyang Technological University (NTU) in 1987, and currently she is an associate professor in the School of Electrical & Electronic Engineering. Her research interests are in CMOS and bipolar IC design, in both the analog/mixed signal and digital fields, as well as design automation.

Kei Tee Tiew earned his B.Eng. (Electrical) degree from the National University of Singapore in 1996, and the DIC and Ph.D. degrees from the Imperial College London, UK in 2002.

He worked as an SRAM and DRAM yield and process integration engineer in Chartered Semiconductor Manufacturing, Singapore, from 1996 to 1998. Since 2003, he has been working as an assistant professor in the School of Electrical and Electronic Engineering, Nanyang Technological University in Singapore. His research interests include analog, mixed-signal, and signal processing IC design.

Liang Mong Koh received his B.Sc. degree in electrical engineering science in 1978 and his Ph.D. degree in 1984.

He was with GEC Traction Pte Ltd (UK) from 1978 to 1980 as an engineer working on microprocessor-based automatic test systems. He joined the University of Manchester Institute of Science and Technology (UMIST), after leaving GEC, as a teaching assistant/research assistant, working on ultrasonic noninvasive measurement techniques. He joined Nanyang Technological Institute in 1984 as a lecturer in the school of EEE. He is currently an associate professor with Nanyang Technical University, Singapore. His current research interests are in ultrasound NDT and medical ultrasound imaging.